

Distributed Sensing and Centric Computing via FMCW Waveform in Wireless Sensor Network

Linlong Wu*, Kunwar Pritiraj Rajput*, Yuan Liu*, Bhavani Shankar*

*Interdisciplinary Center for Security, Reliability and Trust (SnT), University of Luxembourg

Abstract—Wireless Sensor Networks (WSNs) are widely used for environmental sensing, where numerous low-complexity sensors are deployed to collect and partially process measurements. The data is then transmitted to a computing center for information fusion and estimation. Integrated Sensing and Communications (ISAC) is a recent approach that enables simultaneous sensing and data transmission by designing the waveform, architecture, and protocol. This approach has the potential to improve real-time computing and spectral utilization in WSNs. In this paper, we propose a frequency-modulated continuous-wave (FMCW)-based waveform for ISAC, which is cheaper and more suitable for WSNs than other waveforms. We use a pulse-by-pulse modulation scheme to embed communication symbols across all pulses, minimizing the averaged mean square error (AMSE) of these symbols. Additionally, we design the combiner matrix of the computing center in the presence of channel uncertainty. Numerical experiments are conducted to evaluate the effectiveness of the proposed approach.

Index Terms—FMCW, integrated sensing and communications, wireless sensor network, target estimation

I. INTRODUCTION

The Internet of Things (IoT) has revolutionized the way devices with sensing, computation, and communication capabilities interact and coordinate, paving the way for applications such as smart cities and industry 4.0. At the heart of this transformation lies wireless sensor networks (WSNs), which serve as the foundation of IoT by facilitating communication and sensing among a large number of distributed sensors [1], [2]. Typically, the traditional approach of dividing the sensing-communication process into separate stages results in decreased real-time performance and resource utilization.

To address these limitations, the integrated sensing and communication (ISAC) technique has emerged as a promising solution in the context of beyond 5G (B5G) and 6G technologies. ISAC enables simultaneous sensing and communication in the same spectrum by cleverly designing dual-function waveforms, such as orthogonal frequency-division multiplexing (OFDM)-based waveforms. Numerous studies in the open literature have explored the use of OFDM-based waveforms for ISAC. To name a few, the OFDM-based dual-function waveform design considered in [3] boils down to the digital and analog precoding design corresponding to the double-phase-shifter structure. In [4], to achieve a favorable performance trade-off between radar and communications, the powers of OFDM subcarriers are optimized in a time-frequency region of interest. The recent work [5] proposes a method, by dividing the OFDM subcarriers into shared and private ones, to obtain coarse angle estimates first and then

fine-tunes the estimates on the private subcarriers. It is worth mentioning that the OFDM signals have been applied in WSNs [6]–[8] which primarily focused on data transmission and estimation.

The emerging ISAC technology has also been anticipated to be applied in the WSN as clearly stated in the recent survey [9]. Nevertheless, WSN applications have unique characteristics that differentiate them from traditional cellular communication systems and require tailored solutions for ISAC. First, WSNs often have massive sensor deployments with limited capabilities per sensor to keep costs low, such as single antennas and simple receivers. Second, the data transmitted between sensors and the computing center is frequent and lightweight, such as in target localization where only target coordinates need to be sent. These factors make frequency-modulated continuous-wave (FMCW) waveform a suitable candidate for many WSN scenarios. There have been some studies in the literature exploring the use of FMCW waveform for ISAC in different scenarios. In [10], the index modulated FMCW waveform on a sparse array is proposed. The work [11] studied the phase coded FMCW analytically and verified its efficacy for sensing and communication purposes experimentally.

In this paper, we investigate the usage of FMCW-based waveform for ISAC in the context of WSNs. Specifically, we propose a system where sensors emit pulse trains, with each pulse being a FMCW signal embedded with communication symbols for simultaneous data transmission. To enhance communication performance, the inter-pulse modulation and the combiner at the computing center are also jointly designed, which is mathematically formulated as minimization of average mean squared error (MSE). Correspondingly, an alternating method is derived, in which each subproblem can be solved optimally with closed form solutions.

II. INFORMATION-EMBEDDED FMCW AND ISAC MODEL

As shown in Fig. 1, we consider an ISAC system for the WSN application such as target estimation, where M sensors will illuminate the target and communicate with a computing center. Each sensor is assumed to be low-cost and lightweight-computing, and hence a single antenna is equipped for transmitting and receiving signals. In the transmit signals, the information is embedded and captured by the computing center, which is equipped with N_c antennas.

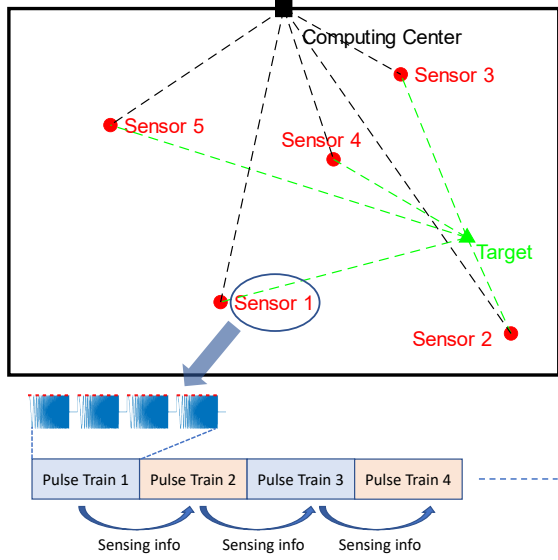


Fig. 1. ISAC in the IoT Application.

A. Information-Embedding FMCW Pulses

The m -th sensor emits the FMCW signal, and its baseband form is defined as

$$u_m(t) = \text{rect}\left(\frac{t - T_{PRI}/2}{T_{PRI}}\right) e^{j\beta_m t^2}, \quad (1)$$

where T_{PRI} is the pulse repetition interval (PRI) and β_m is the chirp rate, $\text{rect}(\cdot)$ represents the rectangular envelope centered at $t = T_{PRI}/2$ with the width T_{PRI} . Assuming that K pulses will be transmitted by the m -th sensor in a single coherent processing interval (CPI), which is given by

$$s_m(t) = \sum_{k=0}^{K-1} c_m x_m[k] u_m(t - kT_{PRI}) e^{j2\pi f_c t}, \quad (2)$$

where f_c is the carrier frequency. In light of pulse agility, a means to incorporate a communication function into the radar emission, we modulate the transmit waveform on a pulse-to-pulse basis by $c_m x_m[k]$, $\forall k = 0, \dots, K-1$, and c_m is known to the sensor as the communication symbol to be sent to the computing center and is encoded on all the K pulses.

B. Sensing Model

Considering the moving target is with range R_m and velocity ν_m with respect to the m -th sensor, the received echo at

the m -th sensor is

$$\begin{aligned} r_m(t) &= \sigma_m s_m(t - \tau_m) + \sum_{m' \neq m} \sigma_{m'} s_{m'}(t - \tau_{m'}) \\ &= \sigma_m \sum_{k=0}^{K-1} c_m x_m[k] u_m(t - kT_{PRI} - \tau_m) e^{j2\pi f_c (t - \tau_m)} + \\ &\quad \sum_{m' \neq m} \sum_{k=0}^{K-1} \sigma_{m'} c_{m'} x_{m'}[k] u_{m'}(t - kT_{PRI} - \tau_{m'}) e^{j2\pi f_c (t - \tau_{m'})}, \end{aligned} \quad (3)$$

where $\tau_m = \frac{2R_m}{c} + \frac{2\nu_m t}{c} = \tau_{m,r} + \tau_{m,d}$. After the downconversion, the baseband signal is

$$\begin{aligned} y_m(t) &= r_m(t) e^{-j2\pi f_c t} \\ &= \sigma_m c_m \sum_{k=0}^{K-1} x_m[k] u_m(t - kT_{PRI} - \tau_m) e^{-j2\pi f_c \tau_m} + \\ &\quad \sum_{m' \neq m} \sigma_{m'} c_{m'} \sum_{k=0}^{K-1} x_{m'}[k] u_{m'}(t - kT_{PRI} - \tau_{m'}) e^{-j2\pi f_c \tau_{m'}}, \end{aligned} \quad (4)$$

which is further dechirped by mixing with the source chirp to generate the intermediate-frequency signal

$$\begin{aligned} z_m(t) &= \sigma_m c_m \sum_{k=0}^{K-1} x_m[k] e^{-j2\pi \tau_m [\beta_m (t - kT_{PRI}) + f_c]} + \\ &\quad \sum_{m' \neq m} \sigma_{m'} c_{m'} \sum_{k=0}^{K-1} x_{m'}[k] e^{-j2\pi \tau_{m'} [\beta_m (t - kT_{PRI}) + f_c]}. \end{aligned} \quad (5)$$

Therefore, the receiver output for each pulse will be a function of both fast and slow time and can be written as

$$\begin{aligned} z_m(n, k) &= \sigma_m c_m x_m[k] e^{-j2\pi (\beta_m \tau_{m,r} + f_{m,d}) \frac{n}{f_s}} e^{-j2\pi f_{m,d} k T_{PRI}} + \\ &\quad \sum_{m' \neq m} \sigma_{m'} c_{m'} x_{m'}[k] e^{-j2\pi (\beta_m \tau_{m',r} + f_{m',d}) \frac{n}{f_s}} e^{-j2\pi f_{m',d} k T_{PRI}} \\ &\approx \sigma_m c_m x_m[k] e^{-j2\pi \beta_m \tau_{m,r} \frac{n}{f_s}} e^{-j2\pi f_{m,d} k T_{PRI}} + \\ &\quad \sum_{m' \neq m} \sigma_{m'} c_{m'} x_{m'}[k] e^{-j2\pi \beta_m \tau_{m',r} \frac{n}{f_s}} e^{-j2\pi f_{m',d} k T_{PRI}} \end{aligned} \quad (6)$$

where $t = \frac{n}{f_s} + kT_{PRI}$, f_s is the sampling frequency, $n = 1, 2, \dots, N_s$ with N_s being the number of samples f_s in one chirp.

Remark 1: The first term in equation (6) accounts for the target range-Doppler information with respect to the m -th sensor while the other terms are the interference caused by other sensors. After applying the 2D-FFT on the data matrix $z_m(n, k)$, the range-Doppler image will contain M target points. Generally, The true target information can be inferred correctly at the computing center by considering all range-Doppler information of all sensors.

Remark 2: To eliminate the above-mentioned interference perfectly, it is accessible to incorporate the time division multiple access (TDMA) techniques [12]. Since all the sensors are single-antenna, applying the TDMA on all distributed sensors will inherently avoid the transmit power loss in the TDMA MIMO radar considered in [12].

C. Communication Model

For the communication model, after the downconversion and dechirp, by the combiner \mathbf{A} , the estimate of the symbols $\{c_m\}_{m=1}^M$ is modeled as

$$\hat{\mathbf{c}}_t = \mathbf{A}^H \left(\sum_{m=1}^M \mathbf{h}_m s_m(t) + \mathbf{n}_c(t) \right) \in \mathbb{C}^{M \times 1}, \quad (7)$$

where \mathbf{A} is the combiner, and \mathbf{h}_m is the channel vector from the m -th sensor to the EC, and $\mathbf{n}_c(t)$ is the Gaussian noise with $\mathbf{n}_c(t) \sim \mathcal{N}(\mathbf{0}, \delta_n^2 \mathbf{I})$.

Given that the goal is to estimate $\mathbf{c} = [c_1, \dots, c_M]^T$ from the K received samples $\{\hat{\mathbf{c}}_k\}_{k=1}^K$, we can formulate the model as

$$\hat{\mathbf{c}} = \mathbf{A}^H \sum_{k=1}^K \left(\sum_{m=1}^M \mathbf{h}_m c_m x_m[k] + \mathbf{n}_c[k] \right) \in \mathbb{C}^{M \times 1}, \quad (8)$$

where $\hat{\mathbf{c}} = [\hat{c}_1, \dots, \hat{c}_M]^T$ is the estimate of \mathbf{c} , which implies that \mathbf{A} essentially combine all signals and yield the average of $\{\hat{\mathbf{c}}_k\}$. To consider the channel uncertainty, we further model \mathbf{h}_m as

$$\mathbf{h}_m = \mathbf{h}_m^c + \Delta \mathbf{h}_m, \quad (9)$$

where $\Delta \mathbf{h}_m \sim \mathcal{N}(\mathbf{0}, \nu_m^2 \mathbf{I})$ being Gaussian channel uncertainty independent with $\mathbf{n}_c(t)$.

This model can be expressed as

$$\hat{\mathbf{c}} = \mathbf{A}^H \bar{\mathbf{H}} \mathbf{X} \mathbf{c} + \mathbf{A}^H \Delta \mathbf{H} \mathbf{X} \mathbf{c} + \mathbf{A}^H \tilde{\mathbf{n}}, \quad (10)$$

where $\mathbf{X} = \text{Diag}(\mathbf{x}_1^T \mathbf{1}, \dots, \mathbf{x}_M^T \mathbf{1})$, $\bar{\mathbf{H}} = [\mathbf{h}_1, \dots, \mathbf{h}_M]$, $\Delta \mathbf{H} = [\Delta \mathbf{h}_1, \dots, \Delta \mathbf{h}_M]$, $\mathbf{c} = [c_1, \dots, c_M]^T \sim \mathcal{N}(\mathbf{0}, \delta_c^2 \mathbf{I})$ and $\tilde{\mathbf{n}} = \sum_{k=1}^K \mathbf{n}_c[k]$ which follows $\tilde{\mathbf{n}} \sim \mathcal{N}(\mathbf{0}, K \delta_n^2 \mathbf{I})$. It is noted that the communication symbols \mathbf{c} is the estimate of target location and radial velocity at previous round, which will be received in the computing center for estimation refinement. For example, when all the estimated ranges are collected in the computing center, the target location can be refined in the sense of minimizing MSE.

III. PROBLEM FORMULATION AND SOLVING APPROACH

A. Problem Formulation

Given the channel uncertainty $\Delta \mathbf{H}$, the MSE of the communication symbols \mathbf{c} is

$$\text{MSE}(\Delta \mathbf{H}) = \text{Tr} \left(\mathbb{E} \left[(\hat{\mathbf{c}} - \mathbf{c})(\hat{\mathbf{c}} - \mathbf{c})^H \right] \right), \quad (11)$$

and further, the average MSE is defined as

$$\text{AMSE} = \mathbb{E}[\text{MSE}(\Delta \mathbf{H})]. \quad (12)$$

The derivation is straightforward and thus omitted, and the final expression is

$$\begin{aligned} & \text{AMSE} \\ &= \delta_c^2 \text{Tr} \left(\mathbf{A}^H \bar{\mathbf{H}} \mathbf{X} \mathbf{X}^H \bar{\mathbf{H}}^H \mathbf{A} \right) \\ & \quad - \delta_c^2 \text{Tr} \left(\mathbf{A}^H \bar{\mathbf{H}} \mathbf{X} + \mathbf{X}^H \bar{\mathbf{H}}^H \mathbf{A} \right) \\ & \quad + \left[\delta_c^2 \text{Tr}(\mathbf{V} \mathbf{X} \mathbf{X}^H) + K \delta_n^2 \right] \text{Tr}(\mathbf{A}^H \mathbf{A}) + \delta_c^2 M, \end{aligned} \quad (13)$$

where $\mathbf{V} = \text{Diag}([\nu_1^2, \dots, \nu_M^2])$.

Thus, the problem is formulated as the minimization of AMSE

$$\begin{aligned} & \text{minimize}_{\mathbf{A}, \{\mathbf{x}_m\}} \text{Tr} \left(\mathbf{A}^H \bar{\mathbf{H}} \mathbf{X} \mathbf{X}^H \bar{\mathbf{H}}^H \mathbf{A} - \mathbf{A}^H \bar{\mathbf{H}} \mathbf{X} + \mathbf{X}^H \bar{\mathbf{H}}^H \mathbf{A} \right) \\ & \quad + \left(\text{Tr}(\mathbf{V} \mathbf{X} \mathbf{X}^H) + K \frac{\delta_n^2}{\delta_c^2} \right) \text{Tr}(\mathbf{A}^H \mathbf{A}) \\ & \text{subject to } \|\mathbf{x}_m\|^2 = P_m, \forall m = 1, \dots, M \\ & \quad \|\mathbf{A}\|_F^2 = P_c. \end{aligned} \quad (14)$$

The problem is nonconvex and variable-coupled in the objective function. In addition, from the formulation, we can see that optimizing pulse modulation \mathbf{x}_m can improve the AMSE performance while its effect on sensing is vague as shown in equation (6).

B. Alternating Optimization

To solve this problem, we adopt the alternating optimization method. For the fixed (\mathbf{X}, \mathbf{p}) , the subproblem of \mathbf{A} is

$$\begin{aligned} & \text{minimize}_{\mathbf{A}} \text{Tr} \left(\mathbf{A}^H \bar{\mathbf{H}} \mathbf{X} \mathbf{X}^H \bar{\mathbf{H}}^H \mathbf{A} - \mathbf{A}^H \bar{\mathbf{H}} \mathbf{X} + \mathbf{X}^H \bar{\mathbf{H}}^H \mathbf{A} \right) \\ & \quad + \left(\text{Tr}(\mathbf{V} \mathbf{X} \mathbf{X}^H) + K \frac{\delta_n^2}{\delta_c^2} \right) \text{Tr}(\mathbf{A}^H \mathbf{A}). \end{aligned} \quad (15)$$

The above problem is an unconstrained quadratic convex problem in terms of the combiner matrix \mathbf{A} , and hence the optimal solution can be obtained by differentiating the objective function with respect to \mathbf{A} and setting it equal to zero. It yields the closed-form expression for the optimal MSE combining matrix as

$$\mathbf{A} = \left(\bar{\mathbf{H}} \mathbf{X} \mathbf{X}^H \bar{\mathbf{H}}^H + \text{Tr} \left(\mathbf{V} \mathbf{X} \mathbf{X}^H + K \frac{\delta_n^2}{\delta_c^2} \right) \mathbf{I} \right)^{-1} \bar{\mathbf{H}} \mathbf{X}. \quad (16)$$

For the fixed \mathbf{A} , the subproblem of (\mathbf{X}, \mathbf{p}) is

$$\begin{aligned} & \text{minimize}_{\{\mathbf{x}_m\}} \text{Tr}(\mathbf{X}^H \mathbf{T} \mathbf{X}) - 2\Re \left\{ \text{Tr}(\mathbf{G}^H \mathbf{X}) \right\} \\ & \text{subject to } \|\mathbf{x}_m\|^2 = P_m, \forall m = 1, \dots, M. \end{aligned} \quad (17)$$

where $\mathbf{T} = \bar{\mathbf{H}}^H \mathbf{A} \mathbf{A}^H \bar{\mathbf{H}} + \text{Tr}(\mathbf{A}^H \mathbf{A}) \mathbf{V}$ and $\mathbf{G} = \bar{\mathbf{H}}^H \mathbf{A}$.

Recall that $\mathbf{X} = \text{Diag}(\mathbf{x}_1^T \mathbf{1}, \dots, \mathbf{x}_M^T \mathbf{1})$, the objective function of problem (17) can be expressed as

$$\begin{aligned} & \text{Tr}(\mathbf{X}^H \mathbf{T} \mathbf{X}) - 2\Re \left\{ \text{Tr}(\mathbf{G}^H \mathbf{X}) \right\} \\ &= \sum_{m=1}^M t_m \mathbf{x}_m^H \mathbf{1} \mathbf{1}^H \mathbf{x}_m + \mathbf{x}_m^H \mathbf{g}_m + \mathbf{g}_m^H \mathbf{x}_m \end{aligned} \quad (18)$$

TABLE I
SENSOR CONFIGURATIONS

Configurations	Values
Central frequency f_c [GHz]	60
Bandwidth B [GHz]	1.8
FMCW slope β [MHz/ μ s]	30
pulse repetition interval T_{PRI} [μ s]	60
pulse repetition count K	128
Sampling rates f_s [MHz]	10
Fast time sampling number N_s	256
Location of Sensor 1 [m]	(1, 1)
Location of Sensor 2 [m]	(4, 8)
Location of Sensor 3 [m]	(8, 0)

where t_m is the m -th diagonal element of \mathbf{T} , $\mathbf{g}_m = -g_m \mathbf{1}$ with g_m being the m -th diagonal element of \mathbf{G} . Thus, problem (17) can be decoupled to be M independent problem as

$$\begin{aligned} & \underset{\mathbf{x}_m}{\text{minimize}} && t_m \mathbf{x}_m^H \mathbf{1} \mathbf{1}^H \mathbf{x}_m + \mathbf{x}_m^H \mathbf{g}_m + \mathbf{g}_m^H \mathbf{x}_m \\ & \text{subject to} && \mathbf{x}_m^H \mathbf{x}_m = P_m, \end{aligned} \quad (19)$$

By setting the gradient of the Lagrangian equal to zero, we have

$$\mathbf{x}_m = -\frac{1}{2} (t_m \mathbf{1} \mathbf{1}^H + \rho_m \mathbf{I})^{-1} \mathbf{g}_m, \quad (20)$$

where ρ_m is the Lagrange multiplier. Substituting it into the constraint and then have

$$\frac{1}{4} \mathbf{g}_m^H (t_m \mathbf{1} \mathbf{1}^H + \rho_m \mathbf{I})^{-1} (t_m \mathbf{1} \mathbf{1}^H + \rho_m \mathbf{I})^{-1} \mathbf{g}_m = P_m \quad (21)$$

Denote the EVD of $t_m \mathbf{1} \mathbf{1}^H$ by $\mathbf{U}^H \mathbf{\Phi} \mathbf{U}$, where $\mathbf{\Phi} = \text{Diag}([t_{m,1}, \dots, t_{m,K}])$ with

$$t_{m,k} = \begin{cases} K t_m & k = 1 \\ 0 & k \neq 1, \end{cases}$$

then equation (21) becomes, defining $\tilde{\mathbf{g}}_m = \mathbf{U} \mathbf{g}_m$,

$$\frac{1}{4} \tilde{\mathbf{g}}_m^H (\mathbf{\Phi} + \rho_m \mathbf{I})^{-1} (\mathbf{\Phi} + \rho_m \mathbf{I})^{-1} \tilde{\mathbf{g}}_m = p_m, \quad (22)$$

which can be further expressed as

$$g(\rho_m) = \frac{1}{4} \sum_{k=1}^K \left| \frac{\tilde{g}_{m,k}}{t_{m,k} + \rho_m} \right|^2 - P_m = 0, \quad (23)$$

where $\tilde{g}_{m,k}$ is the k -th element of $\tilde{\mathbf{g}}_m$. Similarly, $g(\rho_m)$ is monotonically decreasing and its root can be uniquely found by bisection, following which we obtain the optimal \mathbf{x}_m . Therefore, $g(\mu)$ is monotonically decreasing in the possible region of solution, and any local solution is guaranteed to exist and be unique, which can be found by bisection and Newton's method.

IV. SIMULATION RESULTS

In the simulation section, we will evaluate the performance of sensing and communications by the proposed ISAC approach. The size of the whole test area is 10m by 10m. The target location is randomly generated in the whole area and its velocity is a random value within 5 m/s. The parameters

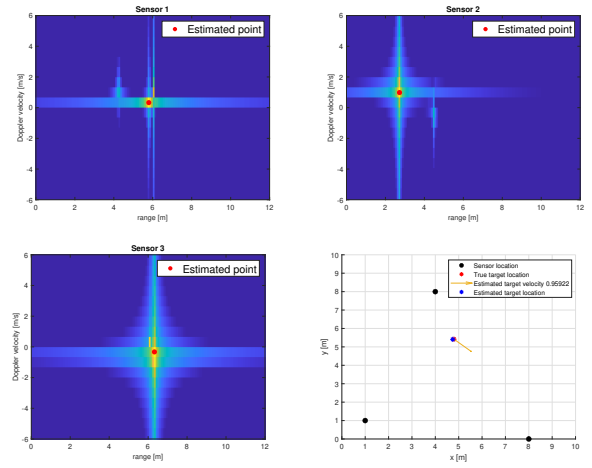


Fig. 2. Case 1: Sensing performance and target estimation

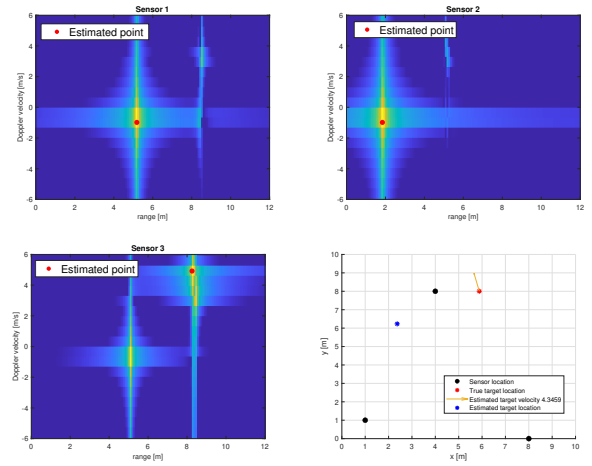


Fig. 3. Case 2: Sensing performance and target estimation

on FMCW pulse trains and testing scenarios are summarized in Table I. Unless otherwise specified, the parameters utilized in all simulation results remain consistent.

In Fig. 2, we present the sensing results on each sensor by conducting the 2D-FFT on the receiving data for one pulse train. We can see that the largest range-Doppler responses of all sensors correspond to the target location and projected radial velocity. After sending the sensing results to the computing center, the target is estimated accurately.

Further, we consider another scenario where the target is far away from one sensor as shown in Fig 3. It is observed that the possible target location by sensor 1 is false, which leads to the false estimation at the center by TOA localization.

Comparing the two examples, we find that the target location has a non-negligible influence on the estimation performance. We conduct a Monte-Carlo experiment, where we generate the target location randomly for the central region marginal region (i.e. inside and outside of the envelope defined by the sensors). The result is presented in Fig. 5. It implies that increasing the number of sensors and proper placement could

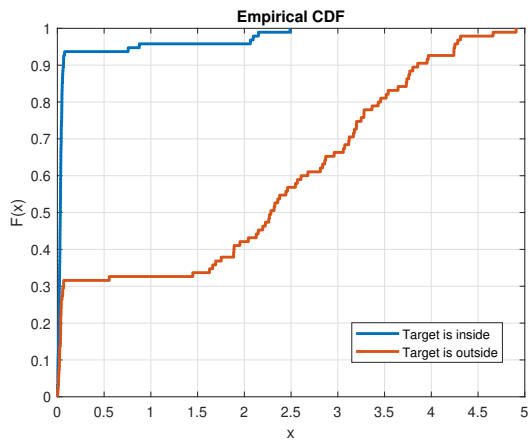


Fig. 4. Monte-Carlo Experiment on localization error for central and marginal regions

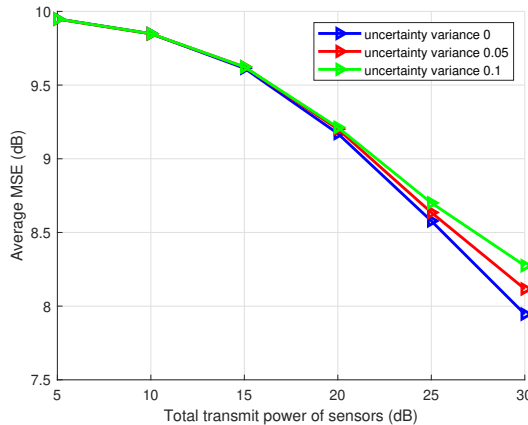


Fig. 5. Monte-Carlo Experiment on average MSE for different channel uncertainty variances.

be a solution to improve the overall performance as studies in [13].

In Fig. 5, we have plotted the communication MSE as a function of the total transmit power budget of the WSN. It can be readily observed that, as expected, with an increase in the total transmit power budget of the sensor, the communication MSE decreases monotonically. Another intuitive observation that can be deduced from the figure is that as the channel uncertainty variance increases in the WSN, the MSE performance tends to deteriorate.

V. CONCLUSIONS

This paper proposed an FMCW-based waveform for ISAC in WSNs. This approach enables simultaneous sensing and data transmission, potentially improving real-time computing and spectral utilization in WSNs. The proposed pulse-by-pulse modulation scheme embeds communication symbols across all pulses, minimizing the AMSE of these symbols. Additionally, our algorithm designed the combiner matrix for the EC in the presence of channel uncertainty. Numerical experiments

are conducted to evaluate the effectiveness of the proposed approach. The results show that the proposed approach is effective and efficient, making it a suitable option for WSNs.

ACKNOWLEDGEMENT

This work was supported in part by the Luxembourg National Research Fund (FNR) through the CORE SPRINGER project under Grant C18/IS/12734677 and in part by ERC AGNOSTIC under Grant EC/H2020/ERC2016ADG/742648.

REFERENCES

- [1] L. Mainetti, L. Patrono, and A. Vilei, "Evolution of wireless sensor networks towards the internet of things: A survey," in *SoftCOM 2011, 19th international conference on software, telecommunications and computer networks*, pp. 1–6, IEEE, 2011.
- [2] Y. Chen, R. S. Blum, and B. M. Sadler, "Optimal quickest change detection in sensor networks using ordered transmissions," in *2020 IEEE 21st International Workshop on Signal Processing Advances in Wireless Communications (SPAWC)*, pp. 1–5, 2020.
- [3] Z. Cheng, L. Wu, B. Wang, M. R. Bhavani Shankar, and B. Ottersten, "Double-phase-shifter based hybrid beamforming for mmWave DFRC in the presence of extended target and clutter," *IEEE Transactions on Wireless Communications*, pp. 1–1, 2022.
- [4] M. F. Keskin, V. Koivunen, and H. Wymeersch, "Limited feedforward waveform design for OFDM dual-functional radar-communications," *IEEE Transactions on Signal Processing*, vol. 69, pp. 2955–2970, 2021.
- [5] Z. Xu and A. Petropulu, "A bandwidth efficient dual-function radar communication system based on a MIMO radar using OFDM waveforms," *IEEE Transactions on Signal Processing*, vol. 71, pp. 401–416, 2023.
- [6] K. P. Rajput, M. F. Ahmed, N. K. Venkatesgoda, A. K. Jagannatham, G. Sharma, and L. Hanzo, "Robust decentralized and distributed estimation of a correlated parameter vector in MIMO-OFDM wireless sensor networks," *IEEE Transactions on Communications*, vol. 69, no. 10, pp. 6894–6908, 2021.
- [7] W. Tang and L. Wang, "Cooperative OFDM for energy-efficient wireless sensor networks," in *2008 IEEE Workshop on Signal Processing Systems*, pp. 77–82, IEEE, 2008.
- [8] Y. Iraqi and A. Al-Dweik, "Efficient information transmission using smart OFDM for IoT applications," *IEEE Internet of Things Journal*, vol. 7, no. 9, pp. 8397–8409, 2020.
- [9] Y. Cui, F. Liu, X. Jing, and J. Mu, "Integrating sensing and communications for ubiquitous IoT: Applications, trends, and challenges," *IEEE Network*, vol. 35, no. 5, pp. 158–167, 2021.
- [10] D. Ma, N. Shlezinger, T. Huang, Y. Liu, and Y. C. Eldar, "FRaC: FMCW-based joint radar-communications system via index modulation," *IEEE journal of selected topics in signal processing*, vol. 15, no. 6, pp. 1348–1364, 2021.
- [11] U. Kumbul, N. Petrov, F. van der Zwan, C. S. Vaucher, and A. Yarovoy, "Experimental investigation of phase coded FMCW for sensing and communications," in *2021 15th European Conference on Antennas and Propagation (EuCAP)*, pp. 1–5, 2021.
- [12] H. Sun, F. Brugi, and M. Lesturgie, "Analysis and comparison of MIMO radar waveforms," in *2014 International Radar Conference*, pp. 1–6, 2014.
- [13] N. Sahu, L. Wu, P. Babu, B. S. MR, and B. Ottersten, "Optimal sensor placement for source localization: A unified admm approach," *IEEE Transactions on Vehicular Technology*, vol. 71, no. 4, pp. 4359–4372, 2022.